International Journal of Fracture **58:** 285–304, 1992.

Numerical solutions of the singular integral equations in the crack analysis using the body force method

NAO-AKI NODA and KAZUHIRO ODA
Department of Mechanical Engineering, Kyushu Institute of Technology, Kitakyushu 804, Japan

Received 15 February 1992; accepted in revised form 8 June 1992

Abstract. In this paper, numerical solutions of the singular integral equations of the body force method in the crack problems are discussed. The stress fields induced by 'two kinds of displacement discontinuity' are used as fundamental solutions. Then, the problem is formulated as a hypersingular integral equation with the singularity of the form r^{-2}. In the numerical calculation, two kinds of unknown functions are approximated by the products of the fundamental density function and the Chebyshev polynomials. As examples, the stress intensity factors of the oblique edge crack, kinked crack, branched crack and zig-zag crack are analyzed. The calculation shows that the present method gives accurate results even for the extremely oblique edge crack and kinked crack with extremely short bend which has been difficult to analyze by the previous method using the approximation by the products of the fundamental density function and the stepped functions etc.

1. Introduction

As a result of computer developments, various numerical methods useful for stress analysis have been developed. The body force method (BFM) was originally proposed by Nisitani [1] as a new method for solving the stress problems using a digital computer. This method has been widely applied to the analysis of the stress concentration factors and the stress intensity factors for various notch and crack problems [2]. In solving the two-dimensional crack problems, the body force method uses the stress field due to 'the pair of point force' or 'the displacement discontinuity' in an infinite plate as a fundamental solution. The fundamental stress field has a singularity of the form r^{-2}. The given boundary conditions are satisfied by applying 'the body force doublet' (continuously embedded pairs of point forces) along the prospective boundary of the crack. Therefore, solving the problems is reduced to determining the densities of the body force doublets which are unknown functions at the imaginary boundary. In the numerical solutions of the body force method, the concept of the fundamental density function was originally proposed and the unknown functions have been approximated by the products of the fundamental density functions and the stepped functions [2]. The stress at an arbitrary point can be calculated by superposing the stress field of the fundamental solutions.

On the other hand, the singular integral equation method, which is based on the same principle of the body force method, has generally used the stress field due to an edge dislocation as the fundamental solution [3]. In this method, the crack problem is formulated as an integral equation having a Cauchy-type singularity r^{-1}. In the analysis of the body force method, however, the problem is formulated as an integral equation with higher singularity of the form r^{-2}. The integral equation of this kind has been recently considered by Ioakimidis [4] and Kaya and Erdogan [5]; it has been called the hypersingular integral equation method (HIEM) or the integral equations with strongly singular kernels.

In this paper, numerical solutions of the singular integral equation of the body force method are discussed and the various crack problems are shown to be solved with higher accuracy compared with previous research.

2. Solution of the integral equations of the body force method for the straight crack

Consider a two-dimensional elastic plate with a straight crack as shown in Fig. 1. Normal and shear tractions $p(x)$, $q(x)$ are prescribed on the crack surfaces. The problem may be reduced to the following integral equations where the crack opening displacements, normal and tangential to the crack surface $V_1(\xi)$, $V_2(\xi)$ are to be unknown functions [5]:

$$\begin{aligned}
&\fint_a^b \frac{V_1(\xi)}{(\xi - x)^2}\,d\xi + \int_a^b H_{11}(\xi, x)V_1(\xi)\,d\xi + \int_a^b H_{12}(\xi, x)V_2(\xi)\,d\xi = -\pi\frac{1+\kappa}{2G}p(x),\\
&\fint_a^b \frac{V_2(\xi)}{(\xi - x)^2}\,d\xi + \int_a^b H_{21}(\xi, x)V_1(\xi)\,d\xi + \int_a^b H_{22}(\xi, x)V_2(\xi)\,d\xi = -\pi\frac{1+\kappa}{2G}q(x),
\end{aligned} \tag{1}$$

where G = shear modulus, $\kappa = 3\text{–}4\nu$ (for plane strain), ν = Poisson's ratio.

Here $\fint$ is interpreted in the Hadamard sense by retaining the finite part of the divergent integral and the kernel $H_{ij}(\xi, x)$ $(i, j = 1, 2)$ is a function known to satisfy the boundary condition expected at the crack surface. It should be noted that Eqns. (1) are virtually the boundary conditions which should be satisfied by continuous distribution of 'the two kinds of displacement discontinuity' along the prospective crack site in the elastic plate without a crack [17]. The two kinds of displacement discontinuity are defined in Fig. 2(a). Figure 2(a) shows the discontinuity in the normal direction of facets and the discontinuity in the tangential direction of facets, both having the magnitude $ds \times d\delta$ (ds: the area of $d\Gamma$).

The stress fields due to the displacement discontinuity can be obtained by distributing 'the standard set of force doublet' as shown in Fig. 2(b). We have the relationship between the stresses due to the unit displacement discontinuity σ_{v1}, σ_{v2} and the stresses due to the tension type and shear type force doublets of unit size σ_{pr}, σ_{ps} as shown in (2).

$$\sigma_{v1} = \frac{G(\kappa + 1)}{\kappa - 1}\sigma_{pr}, \quad \sigma_{v2} = G\sigma_{ps}. \tag{2}$$

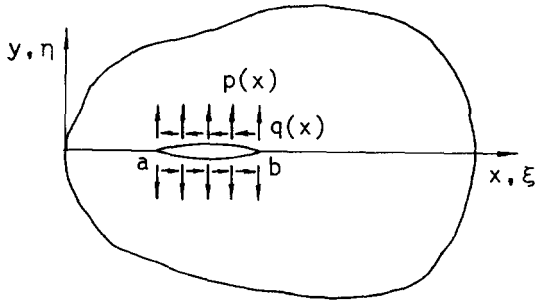

Fig. 1. Elastic plate with a crack.

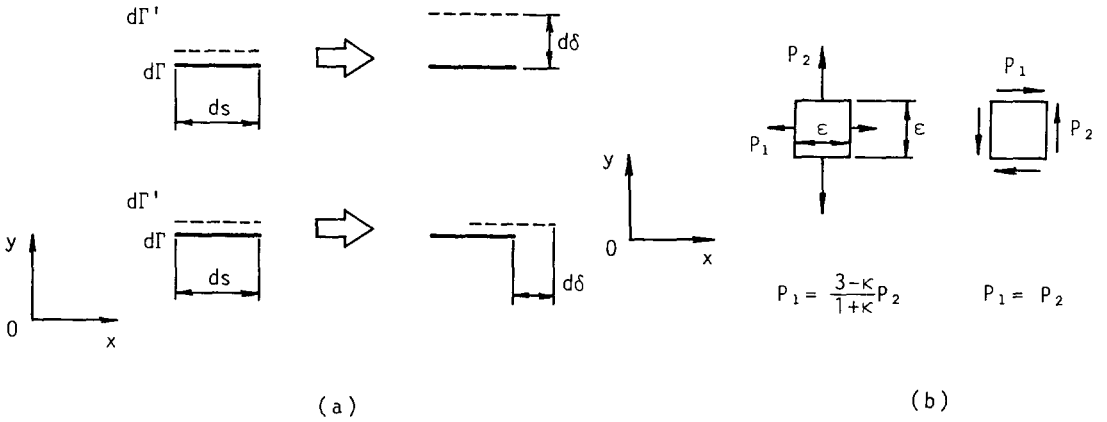

Fig. 2. (a) Two kinds of displacement discontinuity having magnitude of ds × dδ, (b) and two kinds of standard set of force doublet having magnitude of $P_2 \times \varepsilon$.

We have defined the magnitude of a force doublet as follows.

$$T = \lim_{\varepsilon \to 0}(P_2 \times \varepsilon) \quad (P_2 \times \varepsilon = \text{const.}). \tag{3}$$

Using the relationship shown in (2), the integral equations (1) become

$$\begin{aligned} &\int\!\!\!\!\!\!-_a^b \frac{P_1(\xi)}{(\xi - x)^2}\,d\xi + \int_a^b H_{11}(\xi, x)P_1(\xi)\,d\xi + \int_a^b H_{12}(\xi, x)P_2(\xi)\,d\xi = -\pi\frac{(\kappa+1)^2}{2(\kappa-1)}p(x), \\ &\int\!\!\!\!\!\!-_a^b \frac{P_2(\xi)}{(\xi - x)^2}\,d\xi + \int_a^b H_{21}(\xi, x)P_1(\xi)\,d\xi + \int_a^b H_{22}(\xi, x)P_2(\xi)\,d\xi = -\pi\frac{\kappa+1}{2}q(x), \end{aligned} \tag{4}$$

where $P_i(\xi)$ $(i = 1, 2)$ is the density of force doublets which is an unknown function at the imaginary boundary.

In solving the integral equations (4) for the body force method, the imaginary crack line has been divided into M equal intervals and the continuously varying unknown functions have been approximated by the products of the fundamental density function and the stepped function, constant in each interval [2]. Namely, unknown functions $P_1(x)$, $P_2(x)$ in (4) are expressed by

$$P_1(\xi) = t_{1j}\frac{(\kappa+1)^2}{2(\kappa-1)}\sqrt{c^2 - (\xi - d)^2}, \quad P_2(\xi) = t_{2j}\frac{(\kappa+1)^2}{2}\sqrt{c^2 - (\xi - d)^2} \quad (j = 1, 2, \ldots, M), \tag{5}$$

where

$$c = (b - a)/2, \quad d = (a + b)/2 \tag{6}$$

and t_{ij} $(i = 1, 2)$ is the stepped function which is a constant in each interval. The given boundary conditions are satisfied at the mid-point of each interval. We have defined

$$x_j = \frac{b-a}{M}(j - 0.5) + a \quad (j = 1, 2, \ldots, M). \tag{7}$$

In another approach to the solution of the body force method, Isida has used the piecewise linear functions at each interval instead of the stepped functions and the boundary condition has been satisfied by the resultant forces at each interval [7]. Isida has shown that those methods have given results of better accuracy compared with the previous method using the stepped function and the boundary conditions at the mid-point of each interval.

In this study the unknown functions are approximated by using the continuous functions instead of the stepped functions at each interval.

First, normalizing the interval (a, b) of integration by defining

$$r = \frac{2\xi - (b+a)}{b-a}, \quad s = \frac{2x - (b+a)}{b-a}, \tag{8}$$

$$f_i(r) = \frac{2}{b-a} P_i(\xi) \quad (i = 1, 2), \tag{9}$$

the integral equations (4) become

$$\begin{aligned} &\int_{-1}^{1} \frac{f_1(r)}{(r-s)^2}\,dr + \int_{-1}^{1} h_{11}(r,s) f_1(r)\,dr + \int_{-1}^{1} h_{12}(r,s) f_2(r)\,dr = -\pi \frac{(\kappa+1)^2}{2(\kappa-1)} p(s), \\ &\int_{-1}^{1} \frac{f_2(r)}{(r-s)^2}\,dr + \int_{-1}^{1} h_{21}(r,s) f_1(r)\,dr + \int_{-1}^{1} h_{22}(r,s) f_2(r)\,dr = -\pi \frac{\kappa+1}{2} q(s), \end{aligned} \tag{10}$$

where

$$h_{ij}(r,s) = \left(\frac{b-a}{2}\right)^2 H_{ij}(\xi, x) \quad (i, j = 1, 2). \tag{11}$$

In the solution of (10), the unknown function $f_i(r)$ $(i = 1, 2)$ is approximated by the product of the fundamental density function $w_i(r)$ $(i = 1, 2)$ and the Chebyshev polynomial $U_n(r)$

$$w_1(r) = \frac{(\kappa+1)^2}{2(\kappa-1)}\sqrt{1-r^2}, \quad w_2(r) = \frac{\kappa+1}{2}\sqrt{1-r^2}, \tag{12}$$

$$\begin{aligned} &f_1(r) = F_{\mathrm{I}}(r) w_1(r), && F_{\mathrm{I}}(r) \cong \sum_{n=0}^{M-1} a_n U_n(r), \\ &f_2(r) = F_{\mathrm{II}}(r) w_2(r), && F_{\mathrm{II}}(r) \cong \sum_{n=0}^{M-1} b_n U_n(r). \end{aligned} \tag{13}$$

The integral involves a singular term which is evaluated by using the following expression:

$$\int_{-1}^{1} \frac{U_n(r)\sqrt{1-r^2}}{(r-s)^2}\,dr = -\pi(n+1)U_n(s). \tag{14}$$

By substituting from (12) and (13) into (10) and by using (14), the following set of $2M$ linear equations is obtained

$$\begin{aligned}
&\sum_{n=0}^{M-1} [a_n\{-\pi(n+1)U_n(s) + A_n(s)\} + b_n B_n(s)] = -\pi p(s),\\
&\sum_{n=0}^{M-1} [a_n C_n(s) + b_n\{-\pi(n+1)U_n(s) + D_n(s)\}] = -\pi q(s),
\end{aligned} \tag{15}$$

where

$$\begin{aligned}
A_n(s) &= \int_{-1}^{1} h_{11}(r,s)U_n(r)\sqrt{1-r^2}\,dr,\\
B_n(s) &= \frac{\kappa-1}{\kappa+1} \int_{-1}^{1} h_{12}(r,s)U_n(r)\sqrt{1-r^2}\,dr,\\
C_n(s) &= \frac{\kappa+1}{\kappa-1} \int_{-1}^{1} h_{21}(r,s)U_n(r)\sqrt{1-r^2}\,dr,\\
D_n(s) &= \int_{-1}^{1} h_{22}(r,s)U_n(r)\sqrt{1-r^2}\,dr.
\end{aligned} \tag{16}$$

The convenient set of collocation points is given by

$$s_j = \cos\left(\frac{2j+1}{M}\frac{\pi}{2}\right) \quad (j = 0, 1, \ldots, M-1). \tag{17}$$

The unknown coefficients a_n, b_n are determined from (15). The stress intensity factors can be calculated from

$$K_{\mathrm{I}}(b) = F_{\mathrm{I}}(1)\sqrt{\pi\frac{b-a}{2}}, \quad K_{\mathrm{II}}(b) = F_{\mathrm{II}}(1)\sqrt{\pi\frac{b-a}{2}}, \tag{18}$$

3. Solution of the integral equations of the body force method for the intricate crack shape

This section concerns the application of the present method for the solution of the problems with intricate crack shapes. By taking as an example, the kinked crack problem, the method of solution will be illustrated.

3.1. Method of analysis

Consider a kinked crack in an elastic plate as shown in Fig. 3. It consists of the main part whose length is 'a' and the bend part whose length is 'b' inclined by θ to the main part. By superposing the stress fields of a standard set of force doublets on the imaginary crack line, the problem is reduced to the following integral equations.

$$
\begin{aligned}
&\int_d^{d+a} \frac{P_{1A}(\xi_A)}{(\xi_A - x_A)^2}\,d\xi_A + \int_d^{d+a} K_{1A}(\xi_A, x_A)P_{1A}(\xi_A)\,d\xi_A + \\
&+ \int_o^b [k_{1B}(\xi_B, x_A) + K_{1B}(\xi_B, x_A)]P_{1B}(\xi_B)\,d\xi_B + \\
&+ \int_d^{d+a} [k_{2A}(\xi_A, x_A) + K_{2A}(\xi_A, x_A)]P_{2A}(\xi_A)\,d\xi_A + \\
&+ \int_o^b [k_{2B}(\xi_B, x_A) + K_{2B}(\xi_B, x_A)]P_{2B}(\xi_B)\,d\xi_B = -\pi\frac{(\kappa+1)^2}{2(\kappa-1)}p(x_A), \\
&\int_d^{d+a} \frac{P_{2A}(\xi_A)}{(\xi_A - x_A)^2}\,d\xi_A + \int_d^{d+a} K_{2A}(\xi_A, x_A)P_{2A}(\xi_A)\,d\xi_A + \\
&+ \int_o^b [k_{2B}(\xi_B, x_A) + K_{2B}(\xi_B, x_A)]P_{2B}(\xi_B)\,d\xi_B + \\
&+ \int_d^{d+a} [k_{1A}(\xi_A, x_A) + K_{1A}(\xi_A, x_A)]P_{1A}(\xi_A)\,d\xi_A + \\
&+ \int_o^b [k_{1B}(\xi_B, x_A) + K_{1B}(\xi_B, x_A)]P_{1B}(\xi_B)\,d\xi_B = -\pi\frac{\kappa+1}{2}q(x_A),
\end{aligned}
\tag{19}
$$

where the subscripts A and B denote the main and bend part of the crack, respectively. The kernels $k_{ij}(\xi, x)$ $(i = 1, 2,\ j = A, B)$ are stresses due to the standard set of body force doublets in

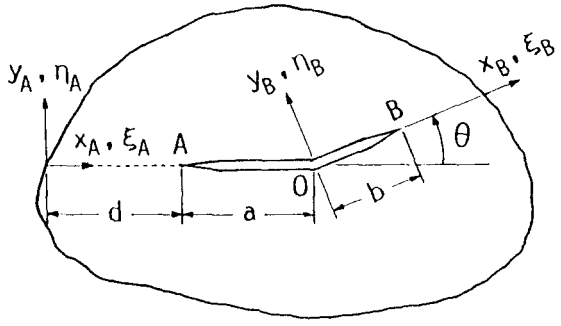

Fig. 3. Elastic plate with a kinked crack.

an infinite plate and the kernels $K_{ij}(\xi, x)$ $(i = 1, 2, j = A, B)$ are functions known to satisfy the boundary conditions except at the crack surface. Equations (19) are corresponding to the boundary equations of the main part. The equations of the bend part can be expressed by exchanging the subscript A in (19) for B.

The intervals of integration are normalized by introduction of the new variables r and s:

$$\begin{aligned} &r_i = (\xi_i - e_i)/L_i, \quad s_i = (x_i - e_i)/L_i, \\ &f_{1i}(r_i) = P_{1i}(\xi_i)/L_i, \quad f_{2i}(r_i) = P_{2i}(\xi_i)/L_i \quad (i = A, B), \end{aligned} \tag{20}$$

where L_A, L_B are some specific length to be determined from the pattern of the fundamental density function. The notations e_A, e_B are the distance from the origin of the $x - y$ coordinate axes. Although there are a few patterns for choosing the fundamental density function, in this section L_A, L_B and e_A, e_B are defined as follows:

$$L_A = (a + b\cos\theta)/2, \quad L_B = b, \quad e_A = d + L_A, \quad e_B = 0. \tag{21}$$

Unknown functions are approximated by the products of the fundamental density functions $w_1(r), w_2(r)$ as shown in (12) and the Chebyshev polynomials $U_n(r)$. Here, $M1$ and $M2$ are the collocation numbers of the main and the bend part of the crack, respectively.

$$\begin{aligned} &f_{1A}(r_A) = F_{\mathrm{I}}^{A}(r_A)w_1(r_A), \quad F_{\mathrm{I}}^{A}(r_A) \cong \sum_{n=0}^{M1-1} a_n U_n(r_A), \\ &f_{2A}(r_A) = F_{\mathrm{II}}^{A}(r_A)w_2(r_A), \quad F_{\mathrm{II}}^{A}(r_A) \cong \sum_{n=0}^{M1-1} b_n U_n(r_A), \\ &f_{1B}(r_B) = F_{\mathrm{I}}^{B}(r_B)w_1(r_B), \quad F_{\mathrm{I}}^{B}(r_B) \cong \sum_{n=0}^{M2-1} c_n U_n(r_B), \\ &f_{2B}(r_B) = F_{11}^{B}(r_B)w_2(r_B), \quad F_{\mathrm{II}}^{B}(r_B) \cong \sum_{n=0}^{M2-1} d_n U_n(r_B). \end{aligned} \tag{22}$$

By substituting from (12), (20), (21) and (22) into (19) and by using (14), we obtain the following system of linear equations for the determination of coefficients a_n, b_n, c_n and d_n.

$$\begin{aligned} &\sum_{n=0}^{M1-1} [a_n\{-\pi(n+1)U_n(s_A) + A_{n1}(s_A)\} + b_n B_{n1}(s_A)] + \\ &\quad + \sum_{n=0}^{M2-1} \{c_n C_{n1}(s_A) + d_n D_{n1}(s_A)\} = -\pi p(s_A), \\ &\sum_{n=0}^{M1-1} [a_n A_{n2}(s_A) + b_n\{-\pi(n+1)U_n(s_A) + B_{n2}(s_A)\}] + \\ &\quad + \sum_{n=0}^{M2-1} \{c_n C_{n2}(s_A) + d_n D_{n2}(s_A)\} = -\pi q(s_A), \\ &\sum_{n=0}^{M1-1} [a_n A_{n3}(s_B) + b_n B_{n3}(s_B)\} + \end{aligned} \tag{23}$$

$$+\sum_{n=0}^{M2-1}[c_n\{-\pi(n+1)U_n(s_B)+C_{n3}(s_B)\}+d_nD_{n3}(s_B)]=-\pi p(s_B),$$

$$\sum_{n=0}^{M1-1}[a_nA_{n4}(s_B)+b_nB_{n4}(s_B)\}+$$

$$+\sum_{n=0}^{M2-1}[c_nC_{n4}(s_B)+d_n\{-\pi(n+1)U_n(s_B)+D_{n4}(s_B)\}]=-\pi q(s_B),$$

where we have defined

$$A_{n1}(s_A)=-\int_m^1\frac{U_n(r_A)}{(r_A-s_A)^2}\sqrt{1-r^2}\,dr_A+$$

$$+\int_{-1}^{m}K_{1A}(r_A,s_A)U_n(r_A)\sqrt{1-r_A^2}\,dr_A,\quad m=\frac{a}{L_A}-1,$$

$$B_{n1}(s_A)=\int_{-1}^{m}[k_{2A}(r_A,s_A)+K_{2A}(r_A,s_A)]U_n(r_A)\frac{\kappa-1}{\kappa+1}\sqrt{1-r_A^2}\,dr_A,$$

$$C_{n1}(s_A)=\int_0^1[k_{1B}(r_B,s_A)+K_{1B}(r_B,s_A)]U_n(r_B)\sqrt{1-r_B^2}\,dr_B, \tag{24}$$

$$D_{n1}(s_A)=\int_0^1[k_{2B}(r_B,s_A)+K_{2B}(r_B,s_A)]U_n(r_B)\frac{\kappa-1}{\kappa+1}\sqrt{1-r_B^2}\,dr_B.$$

$A_{n2}(s_A)\sim D_{n4}(s_B)$ are defined from similar formulas.

3.2. *Discussion on the solution accuracy*

In the case of the analysis of the kinked crack with an extremely short bend, it is well known that the solution accuracy generally goes down as bend length b approaches zero. Hence, we have to give special consideration to the position of the collocation points and the ratio of the collocation point number for the main and the bend part, etc. [8]. In this section, by taking as an example of the tension an infinite plate with the 45° angled kinked crack, as shown in Fig. 4, we will investigate the primary factors which seem to affect the numerical results.

3.2.1. *Effect of the position of the collocation points*

First the collocation points are selected at the same intervals as shown in (25)

$$s_{Bj}=\frac{j}{M2+1}\quad(j=1,2,\ldots,M2,\ 0<s_{Bj}<1). \tag{25}$$

When $b/a<0.1$ in Fig. 4, however, the convergency of the solution goes down and a lot of collocation points are needed to get accurate results. Therefore, the position of the collocation

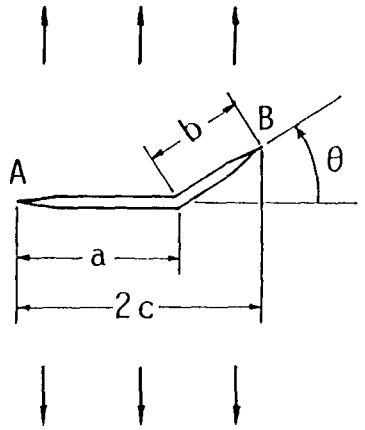

Fig. 4. Tension of an infinite plate with a kinked crack.

points is modified as shown in (26). In using (26), we have more collocation points near the bend point and the crack tip

$$s_{Bj} = \frac{1}{2}\cos\left(\frac{2j-1}{M2}\frac{\pi}{2}\right) \quad (j = 1, 2, \ldots, M2,\ 0 < s_{Bj} < 1). \tag{26}$$

As shown in Table 1, it is found that the position of collocation points has a considerable effect on the numerical calculations and the calculation using the collocation points as shown in (26) gives rapidly converging numerical results.

Table 1. Effect of the position of the collocation points ($\theta = 45°$ in Fig. 4)

b/a	Eq.	$M1$	$M2$	F_{I}^{B}	F_{II}^{B}
0.1	(25)	5	5	0.62308	0.53435
		10	10	0.63066	0.50958
		15	15	0.63116	0.50702
	(26)	5	5	0.63262	0.50713
		10	10	0.63293	0.50753
		15	15	0.63298	0.50651
	Kitagawa et al. [9]			0.634	0.505
0.01	(25)	16	4	0.68209	0.47046
		20	5	0.68675	0.47049
		24	6	0.69170	0.45723
	(26)	16	4	0.73096	0.39338
		20	5	0.73026	0.39262
		24	6	0.73015	0.39219
	Kitagawa et al. [9]			0.732	0.389

3.2.2. Effect of the ratio of the collocation point number $M2/M1$

In the previous analysis of the body force method using such stepped function, it has been found that the ratio of the collocation point $M2/M1$ should be chosen to be nearly equal to the ratio b/a. Therefore, we will consider the effect of $M2/M1$ on the numerical calculation. Table 2 shows the convergency of the dimensionless stress intensity factor for different ratio $M2/M1$. As shown

Table 2. Effect of the ratio of the collocation point number M_2/M_1 ($\theta = 45°$, $b/a = 0.01$ in Fig. 4)

$M2/M1$	$M1$	$M2$	F_{I}^{B}	F_{II}^{B}
	25	5	0.73062	0.39181
0.2	30	6	0.73053	0.39113
	35	7	0.73046	0.39052
	30	3	0.73280	0.38943
0.1	40	4	0.73122	0.38931
	50	5	0.73131	0.38836
	60	3	0.73195	0.38627
0.05	80	4	0.73147	0.38656
	100	5	0.73118	0.38684

in Table 2, in the case that $b/a = 0.01$, the results have enough accuracies even when $M2/M1 = 0.2$.

3.2.3. Effect of the specific length of the fundamental density function

The fundamental density function as shown in (12) is an important concept of the body force method to obtain accurate solutions [2]. In this section, the two kinds of specific length of the fundamental density functions as shown in Fig. 5(a) and (b) are used and both numerical results are compared. The specific length L_A as shown in Fig. 5(a) is defined by (21), and the specific length L_B shown in Fig. 5(b) is defined by

$$L_B = \frac{1}{2}\left(\frac{a}{\cos\theta} + b\right). \tag{27}$$

Table 3 shows the convergency of the dimensionless SIFs for different specific length. As shown in Table 3, the specific length of the fundamental density function does not have much effect on the solution accuracy. Therefore, in the numerical calculations of the other results, the specific length L_A shown in Fig. 5(a) is used.

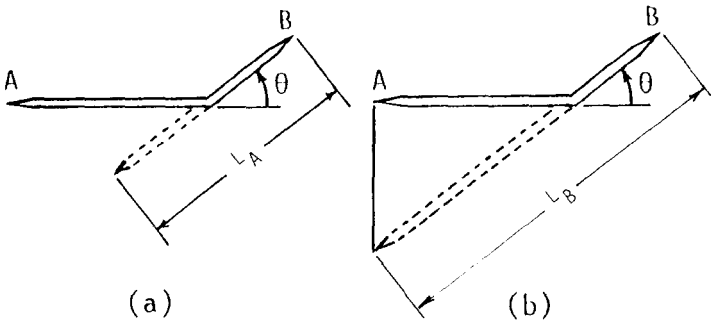

Fig. 5. Specific length of the fundamental density function.

Table 3. Effect of the specific length of the fundamental density function ($\theta = 45°$ in Fig. 3)

$F_{\mathrm{I}}^{B} = K_{\mathrm{I}}/\sigma\sqrt{\pi c}$				
b/a	$M1$	$M2$	L_A	L_B
	12	4	0.6337	0.6337
0.1	18	6	0.6334	0.6334
	24	8	0.6334	0.6330
	9	9	0.5691	0.5691
1.0	11	11	0.5691	0.5691
	13	13	0.5691	0.5691
$F_{\mathrm{II}}^{B} = K_{\mathrm{II}}/\sigma\sqrt{\pi c}$				
b/a	M1	$M2$	L_A	L_B
	12	4	0.5062	0.5061
0.1	18	6	0.5057	0.5057
	24	8	0.5056	0.5052
	9	9	0.6411	0.6411
1.0	11	11	0.6411	0.6411
	13	13	0.6411	0.6411

4. Numerical results and discussion

4.1. Oblique edge crack

The problem of the oblique edge crack in the semi-infinite plate under uniform tension as shown in Fig. 6 has been analyzed by Nisitani [6] and Isida [8] using the body force method. Nisitani has used the stepped function and the boundary conditions have been satisfied at the mid-point of each interval. Isida has used the piecewise linear functions at each interval and the boundary condition has been satisfied by the resultant force at each interval. On the other hand, Hasebe

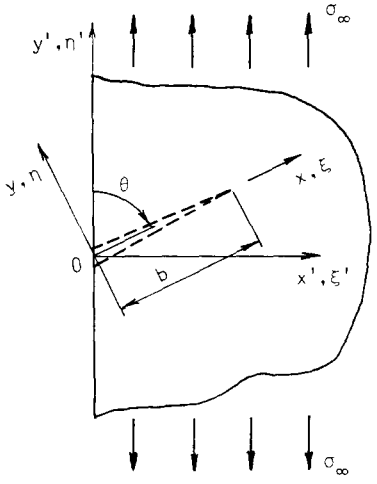

Fig. 6. Oblique edge crack in a semi-infinite plate under uniform tension.

Table 4. Dimensionless SIFs of the oblique edge crack in a semi-infinite plate (Fig. 6).

θ°	Present analysis		Nisitani [6]		Isida [8]		Hasebe [10]	
	F_I	F_{II}	F_I	F_{II}	F_I	F_{II}	F_I	F_{II}
10	0.1621	0.1734					0.162	0.174
15	0.2318	0.2261	0.225	0.228	0.239	0.219	0.232	0.226
20	0.3054	0.2710					0.305	0.271
22.5	0.3436	0.2905			0.335	0.301		
30	0.4625	0.3362	0.461	0.337	0.461	0.338	0.463	0.336
37.5	0.5845	0.3613			0.584	0.362		
40	0.6251	0.3648					0.6251	0.3648
45	0.7049	0.3645	0.705	0.364	0.705	0.364	0.7050	0.3644
50	0.7817	0.3543					0.7818	0.3543
60	0.9201	0.3058	0.920	0.306	0.920	0.306	0.9201	0.3058
67.5	1.0048	0.2474			1.005	0.247		
70	1.0286	0.2243					1.0286	0.2243
75	1.0686	0.1738	1.068	0.174	1.069	0.174		
80	1.0978	0.1186			1.098	0.119	1.0978	0.1186
85	1.1155	0.0601			1.116	0.060		
90	1.1215	0.0000	1.121	0.000	1.121	0.000	1.1215	0.0000

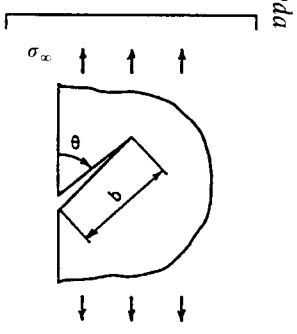

[10] has analyzed this problem by using the rational mapping function and the complex variable method. In Table 4, the stress intensity factors of the oblique edge crack for various values of θ are shown, where F_I and F_{II} are dimensionless SIFs based on $\sigma_\infty\sqrt{\pi b}$. The numerical results obtained by those methods are in close agreement; however, when $\theta < 30°$, each result makes a small difference. Present results are in better agreement with the results by Hasebe than those of Nisitani and Isida. In Table 4, it should be noted that Nisitani's values are obtained by the extrapolation for the results for $M = 32$ and 24.

Table 5 shows the convergency of the numerical results by the present method compared with the results by using the stepped functions. In Table 5, the symbol $\infty(32 - 24)$ designates the extrapolated value using the results of $M = 32$ and $M = 24$ on the basis of the linear relationship between the SIFs and $1/M$. As shown in Table 5, it is found that when increasing the collocation points M, the extrapolated values approach the present results even when $\theta < 30°$. The present method is found to give results of better accuracy and shorter CPU time compared with the previous method using such stepped functions.

In Fig. 7(a)–(c), the expressions of the unknown functions F_I, F_{II} in (13) are compared using the Chebyshev polynomials and the stepped functions (BFM). In the present analysis using the Chebyshev polynomials, the expresion of $M = 20$ and the one of $M = 30$ almost coincide with each other and therefore they seem to express the unknown functions F_I and F_{II} very accurately. On the other hand, when we use the stepped functions to analyze the extremely oblique edge crack ($\theta < 30°$), both expressions of $M = 20$ and 40 don't coincide with the present analysis. However, on increasing the collocation points M, they seem to approach the present analysis.

Table 5. Comparison of the convergence of SIFs (Chebyshev polynomials and stepped function).

$\theta°$	Present analysis			BFM(stepped function)		
	M	F_I	F_{II}	M	F_I	F_{II}
	5	0.70403	0.36557	24	0.70788	0.36106
	10	0.70499	0.36455	32	0.70704	0.36190
	15	0.70488	0.36446	64	0.70583	0.36321
45	20	0.70489	0.36447	96	0.70546	0.36365
	25	0.70490	0.36448	∞(32–24)	0.70453	0.36443
				∞(64–32)	0.70462	0.36452
				∞(96–64)	0.70472	0.36454
	10	0.46260	0.33590	24	0.45300	0.34275
	15	0.46257	0.33620	32	0.45505	0.34122
	20	0.46254	0.33619	64	0.45838	0.33880
30	24	0.46250	0.33617	96	0.45960	0.33795
	30	0.46247	0.33616	∞(32–24)	0.46117	0.33660
				∞(64–32)	0.46171	0.33636
				∞(96–64)	0.46204	0.33626
	20	0.23225	0.22637	24	0.23976	0.22916
	25	0.23184	0.22617	32	0.23611	0.22884
	30	0.23182	0.22616	64	0.23247	0.22780
15	35	0.23181	0.22615	96	0.23175	0.22733
	40	0.23180	0.22614	128	0.23151	0.22707
				∞(32–24)	0.22517	0.22786
				∞(96–64)	0.23031	0.22639
				∞(128–96)	0.23078	0.22628

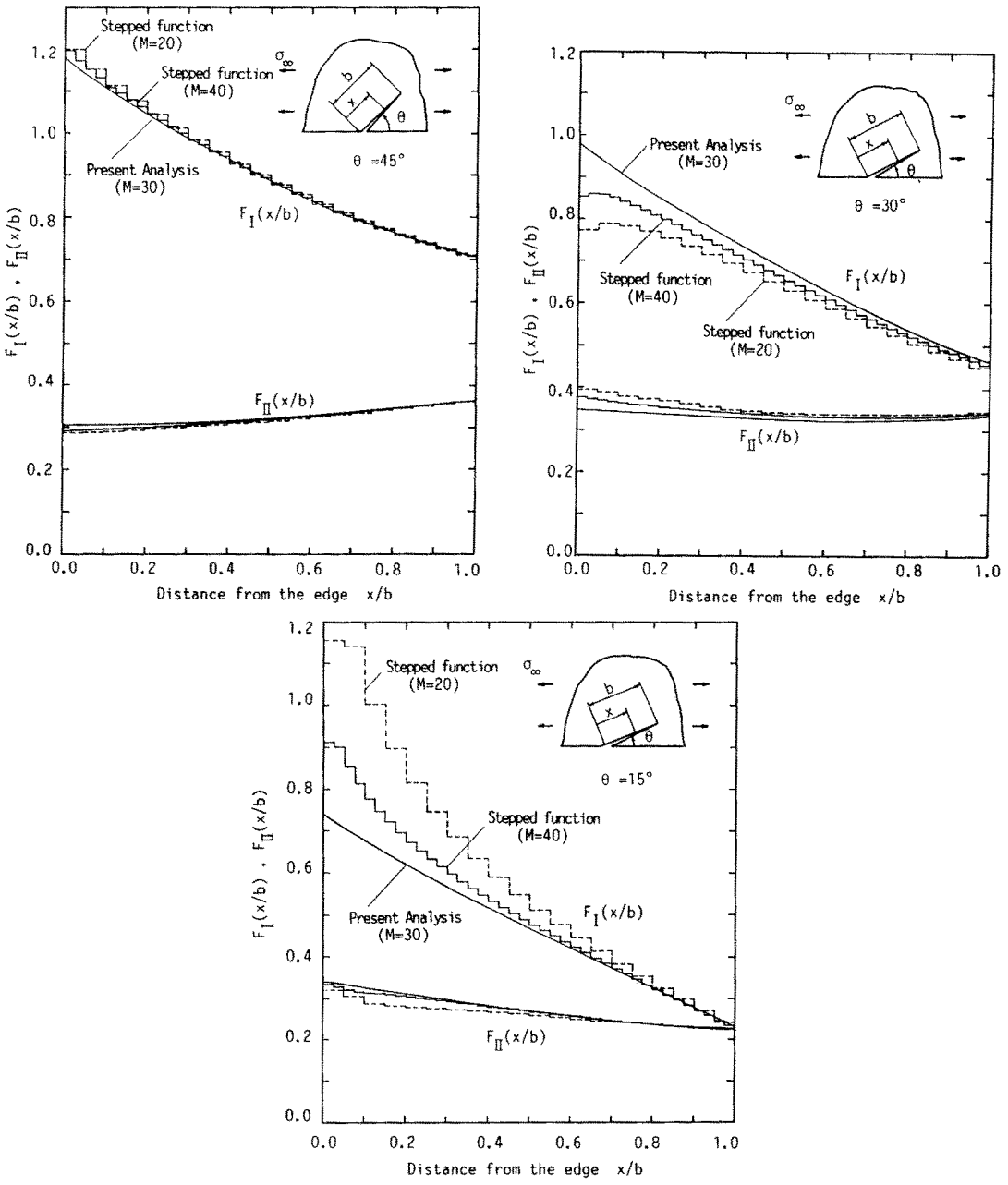

Fig. 7. Comparison of approximation of weight function F_I, F_{II} (Chebyshev polynomials and stepped function). (a) In the case of $\theta = 45°$. (b) In the case of $\theta = 30°$. (c) In the case of $\theta = 15°$.

Figure 8 shows the oblique edge crack subjected to non-linear tractions. The tractions on the crack surface are expressed by

$$P_{yy} = (x/b)^m, \quad P_{xy} = 0,$$
$$P_{xy} = (x/b)^m, \quad P_{yy} = 0.$$

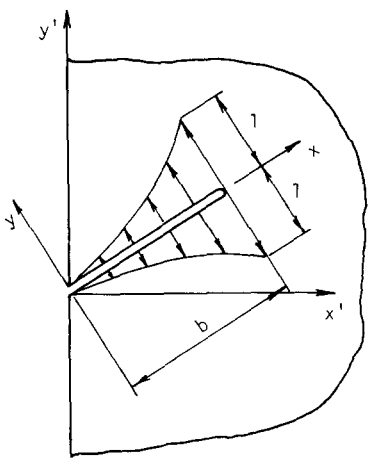

Fig. 8. Oblique edge crack subjected to nonlinear tractions.

Numerical results are given in Table 6 for various m and θ. This problem has been analyzed by Stallybrass [11] (when $\theta = 90°$) and Nisitani and Oda [12] (when $\theta = 30$–$90°$). The present method gives accurate results even for the small angle of θ which has been difficult to calculate by the previous method. The results in Table 6 are useful for estimating the SIFs of the crack emanating from the notch root and the crack in the residual stress field.

4.2. Kinked and branched crack in the infinite plate

The tension problems of kinked crack in the infinite plate as shown in Fig. 4 are analyzed for various values of b/a. The dimensionless factors F_{IB} and F_{IIB} based on $\sigma\sqrt{\pi c}$, where c is the projected length of the total crack, are summarized in Table 7 in comparison with Isida's results [7, 13]. The value of $b/a = 0.000$ in Table 7 is the result of an infinitesimal kinked crack calculated by Kageyama et al. [14]. Both of Isida's results were analyzed by the body force method in which the unknown body force densities are expressed by the piecewise linear functions and the boundary conditions are satisfied by the resultant forces. In [13], unknown body force densities are derived from the solution of the isolated force doublet in a plane with a line crack and can be determined only from the boundary condition along the bend. In this method, because the traction-free condition along the main crack is completely satisfied, a high accurate analysis was actualized compared with the results in [8]. Although the present analysis is based on continuous distributions of body force doublets along the crack of main and bend parts, the results are in close agreement with the results of [13].

The tension problem of the branched crack as shown in Fig. 9 is also analyzed for various values of b/a. Dimensionless factors F_{IB} and F_{IIB} based on $\sigma\sqrt{\pi c}$ in the case of $\theta = 45°$, where c is the projected length of the total crack, are summarized in Table 8 in comparison with the previous values. Present results are in remarkable agreement with the results by Isida and Noguchi [15].

4.3. Kinked and zig-zag edge crack in the semi-infinite plate

A kinked edge crack in a semi-infinite plate subjected to uniform tension is considered, see Fig. 10. This problem in the case of $c2/c1 > 0.1$ has been investigated by Nisitani [6]. The dimensionless factors, normalized with respect to $\sigma\sqrt{\pi c_1/\cos\theta}$, are shown in Table 9.

Table 6. (a) Dimensionless SIFs of edge crack subjected to nonlinear tractions (Fig. 8) (a) In the case of $p_{yy} = (x/b)^m$, $p_{xy} = 0$. case of $p_{yy} = 0$, $p_{xy} = (x/b)^m$.

θ°	m	0		1		2		3		4		5	
		F_I	F_{II}	F_I	F_{II}	F_I	F_{II}	F_I	F_{II}	F_I	F_{II}	F_I	F_{II}
15		5.182	−3.088	2.184	−1.034	1.3329	−0.5167	0.9561	−0.3107	0.7490	−0.2080	0.6197	−0.1494
30		2.325	−1.034	1.1390	−0.3468	0.7749	−0.1747	0.6019	−0.1062	0.5009	−0.0720	0.4345	−0.0523
45		1.587	−0.505	0.8618	−0.1698	0.6239	−0.0864	0.5048	−0.0531	0.4322	−0.0364	0.3828	−0.0267
60		1.290	−0.265	0.7479	−0.0894	0.5614	−0.0458	0.4643	−0.0284	0.4034	−0.0196	0.3611	−0.0145
75		1.159	−0.117	0.6975	−0.0395	0.5336	−0.0204	0.4462	−0.0127	0.3906	−0.0088	0.3513	−0.0065
90		1.1215	0.000	0.6829	0.0000	0.5255	0.0000	0.4410	0.0000	0.3868	0.0000	0.3485	0.0000

Table 6. (b) In the case of $p_{yy} = 0$, $p_{xy} = (x/b)^m$.

θ°	m	0		1		2		3		4		5	
		F_I	F_{II}	F_I	F_{II}	F_I	F_{II}	F_I	F_{II}	F_I	F_{II}	F_I	F_{II}
15		−0.461	1.732	−0.2192	0.9616	−0.1367	0.6953	−0.0968	0.5585	−0.0736	0.4743	−0.0586	0.4168
30		−0.274	1.373	−0.1261	0.7952	−0.0766	0.5922	−0.0531	0.4861	−0.0396	0.4198	−0.0310	0.3739
45		−0.178	1.234	−0.0803	0.7324	−0.0480	0.5545	−0.0328	0.4604	−0.0242	0.4009	−0.0188	0.3593
60		−0.110	1.165	−0.0489	0.7020	−0.0289	0.5366	−0.0196	0.4484	−0.0144	0.3921	−0.0111	0.3526
75		−0.053	1.132	−0.0233	0.6873	−0.0137	0.5280	−0.0092	0.4427	−0.0068	0.3880	−0.0052	0.3494
90		0.000	1.1215	0.0000	0.6829	0.0000	0.5255	0.0000	0.4410	0.0000	0.3868	0.0000	0.3485

Table 7. Dimensionless SIFs of the 45°-kinked crack at the crack tip B in the infinite plate (Fig. 4).

$F_{\mathrm{I}}^{B} = K_{\mathrm{I}}^{B}/\sigma\sqrt{\pi c}$			
b/a	Present analysis	Isida [7]	Isida [13]
0.000[4]	0.791	0.791	0.791
0.005	0.749	—	0.748
0.01	0.731	0.710	0.730
0.1	0.633	0.634	0.633
1.0	0.569	0.569	0.569
$F_{\mathrm{II}}^{B} = K_{\mathrm{II}}^{B}/\sigma\sqrt{\pi c}$			
b/a	Present analysis	Isida [7]	Isida [13]
0.000 [14]	0.324	0.324	0.324
0.005	0.370	—	0.369
0.01	0.388	0.356	0.388
0.1	0.506	0.504	0.505
1.0	0.641	0.641	0.641

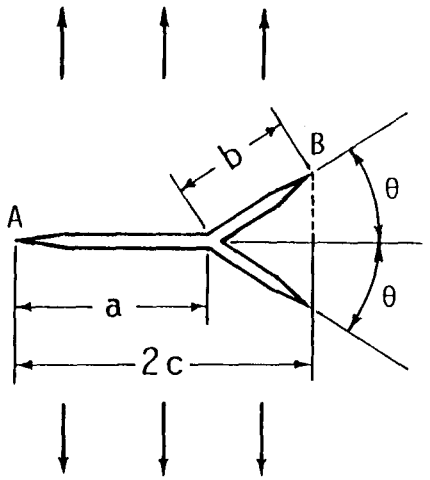

Fig. 9. Tension of an infinite plate with a branched crack.

It is found that present results approach the previous results by Nisitani et al. [16] when $b/a \to 0$.

The problems of zig-zag crack in the semi-infinite plate under tension as shown in Fig. 11 are treated. Here, the number of the branch is N, collocation point number of the bend part is M and total collocation point number is $M \times N$. The dimensionless factors F_{I} and F_{II} are defined as multiples of $\sigma\sqrt{\pi c}$, where c is the total length $N \times a$ of the crack. Values of F_{I} and F_{II} are given in Table 10 for various θ and N. This problem in the case of $\theta = 45°$ has been analyzed by Isida [8]. In Table 10, these results are in close agreement with the results of the straight edge crack (when $N = 1$). Table 11 shows the convergency of the SIFs. Even in the case of the

Table 8. Dimensionless SIFs of the 45°-branched crack (Fig. 9).

$F_{\mathrm{I}}^{B} = K_{\mathrm{I}}^{B}/\sigma\sqrt{\pi c}$		
b/a	Present analysis	Isida [15]
0.02	0.631	0.631
0.03	0.615	0.615
0.05	0.593	0.593
0.1	0.560	0.560
0.5	0.500	0.500
1.0	0.495	
$F_{\mathrm{II}}^{B} = K_{\mathrm{II}}^{B}/\sigma\sqrt{\pi c}$		
b/a	Present analysis	Isida [15]
0.02	0.246	0.246
0.03	0.267	0.267
0.05	0.297	0.297
0.1	0.347	0.347
0.5	0.474	0.474
1.0	0.506	

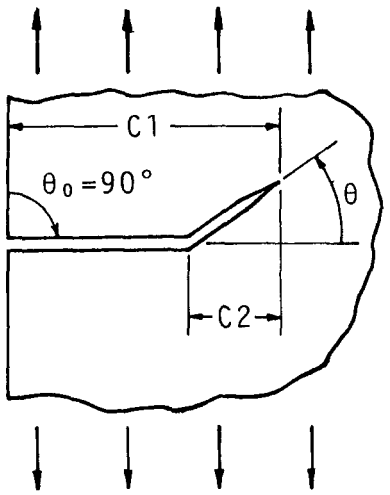

Fig. 10. Tension of a semi-infinite plate with kinked edge crack.

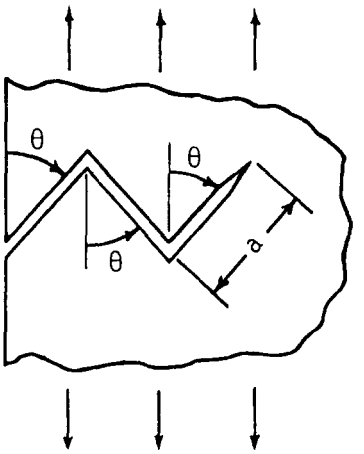

Fig. 11. Tension of a semi-infinite plate with zig-zag crack.

problem with intricate crack shapes, it is found that the convergence of the present numerical method is extremely good.

5. Conclusion

In this paper, the numerical solution of the singular integral equations based on the body force method was investigated. The conclusions are summarized as follows:

Table 9. Dimensionless SIFs of the kinked edge crack (Fig. 10) $F_{I,II} = K_{I,II}/\sigma\sqrt{\pi c_1/\cos\theta}$.

C_2/C_1	θ°	F_I	F_{II}
0.10	60.0	0.467	0.340
	45.0	0.708	0.358
	30.0	0.921	0.295
	15.0	1.068	0.167
0.05	60.0	0.472	0.324
	45.0	0.713	0.342
	30.0	0.924	0.285
	15.0	1.070	0.162
0.03	60.0	0.479	0.313
	45.0	0.717	0.332
	30.0	0.926	0.277
	15.0	1.070	0.158
0.00 [16]	60.0	—	—
	45.0	0.74	0.31
	30.0	0.94	0.25
	15.0	1.07	0.14

Table 10. Dimensionless SIFs of the zig-zag crack (Fig. 11) $F_{I,II} = K_{I,II}/\sigma\sqrt{\pi c}$, $c = N \times a$.

θ°	N	F_I		F_{II}	
		Present analysis	Isida [8]	Present analysis	Isida [8]
30.0	1	0.4625		0.3362	
	2	0.463		0.337	
	3	0.465		0.332	
	4	0.470		0.325	
45.0	1	0.7049	0.705	0.3645	0.365
	2	0.705	0.703	0.365	0.364
	3	0.706	0.704	0.359	0.360
	4	0.708	0.704	0.353	0.355
60.0	1	0.9201		0.3058	
	2	0.920		0.305	
	3	0.920		0.302	
	4	0.921		0.298	

Table 11. Convergence of the SIFs of 45°-zig-zag crack (Fig. 11).

	$N = 3$			$N = 4$	
M	F_I	F_{II}	M	F_I	F_{II}
3	0.7075	0.3621	3	0.7096	0.3561
4	0.7062	0.3606	4	0.7084	0.3544
5	0.7055	0.3601	5	0.7078	0.3539
6	0.7056	0.3598	6	0.7080	0.3536
7	0.7057	0.3596	7	0.7080	0.3534
8	0.7057	0.3595	8	0.7081	0.3533
9	0.7058	0.3594	9	0.7082	0.3532
10	0.7058	0.3593	10	0.7082	0.3532

1. In the analysis of the body force method, the problem is formulated as an integral equation with higher singularity of the form r^{-2}. The present numerical method, in which unknown functions are approximated by the products of the fundamental density functions and the Chebyshev polynomials, was found to give the results of better accuracy and shorter CPU time compared with the previous method using stepped functions etc.
2. The stress intensity factors of the oblique edge crack in the semi-infinite plate were calculated. The present method gave accurate results even for the extremely oblique edge crack which has been difficult to calculate by the previous method.
3. As examples of the problems with the intricate crack shapes, the tension problems of the kinked crack, branched crack and zig-zag crack were treated. Even in the case of the crack with extremely short bend, the accurate numerical results were obtained by selecting a convenient set of collocation points. The present results were in close agreement with previous research. The present method was found to be useful for analyzing exactly various crack problems.

Acknowledgments

The authors wish to thank Prof. H. Nisitani, Prof. S. Harada and Prof. D.H. Chen for valuable advice. The contribution of Chikahiro Masuda in programing some problems is greatly appreciated.

References

1. H. Nisitani, *Journal of the Japan Society of Mechanical Engineers* 70 (1967) 627–635.
2. H. Nisitani, *Mechanics of Fracture* 5, G. C. Sih (ed.), Noordhoff International Publishing, Leyden (1978) 1–68.
3. S. Krenk, *International Journal of Solids and Structures* 11 (1975) 693–708.
4. N.I. Ioakimidis, *Engineering Fracture Mechanics* 26 (1987) 783–788.
5. A.C. Kaya and F. Erdogan, *Quarterly of Applied Mathematics* 45 (1987) 105–122.
6. H. Nisitani, *Transactions of the Japan Society of Mechanical Engineers* 41 (1978) 1103–1111.
7. M. Isida, *Transactions of the Japan Society of Mechanical Engineers* 44 (1978) 1122–1132.
8. Ibid, 45 A (1979) 306–317.
9. H. Kitagawa and R. Yuuki, *Transactions of the Japan Society of Mechanical Engineers* 41 (1975) 1641–1649.
10. N. Hasebe and S. Inohara, *Ingenieur-Archiv* 49 (1980) 51–62.
11. M.P. Stallybrass, *International Journal of Engineering Science* 8 (1970) 351–362.
12. H. Nisitani and Y. Oda, *Transactions of the Japan Society of Mechanical Engineers* 46 (1980) 745–755.
13. M. Isida and T. Nishino, *Engineering Fracture Mechanics* 36 (1990) 697–711.
14. K. Kageyama and H. Okamura, *Transactions of the Japan Society of Mechanical Engineers* 48 A (1982) 783–791.
15. M. Isida and H. Noguchi, *Transactions of the Japan Society of Mechanical Engineers* 49 A (1983) 469–479.
16. H. Nisitani, D. H. Chen and M. Isida, *Transactions of the Japan Society of Mechanical Engineers* 50 A (1984) 341–350.
17. H. Nisitani and D.H. Chen, *The Body Force Method*, Baifukan Publication, Tokyo (1987) (Taisekiryokuhou in Japanese).